HXeI and HXeH in Ar, Kr, and Xe matrices: Experiment and simulation

Cheng Zhu, Keisuke Niimi, Tetsuya Taketsugu, Masashi Tsuge, Akira Nakayama, and Leonid Khriachtchev

Citation: The Journal of Chemical Physics **142**, 054305 (2015); doi: 10.1063/1.4906875
View online: http://dx.doi.org/10.1063/1.4906875
View Table of Contents: http://scitation.aip.org/content/aip/journal/jcp/142/5?ver=pdfcov
Published by the AIP Publishing

HXeI and HXeH in Ar, Kr, and Xe matrices: Experiment and simulation

Cheng Zhu,[1] Keisuke Niimi,[2] Tetsuya Taketsugu,[2] Masashi Tsuge,[1,a)] Akira Nakayama,[3,b)] and Leonid Khriachtchev[1,c)]
[1]*Department of Chemistry, University of Helsinki, P.O. Box 55, FI-00014 Helsinki, Finland*
[2]*Department of Chemistry, Faculty of Science, Hokkaido University, Sapporo 060-0810, Japan*
[3]*Catalysis Research Center, Hokkaido University, Sapporo 001-0021, Japan*

(Received 1 December 2014; accepted 14 January 2015; published online 4 February 2015)

Experimental and theoretical studies of HXeI and HXeH molecules in Ar, Kr, and Xe matrices are presented. HXeI exhibits the H–Xe stretching bands at 1238.0 and 1239.0 cm^{-1} in Ar and Kr matrices, respectively, that are blue-shifted from the HXeI band observed in a Xe matrix (1193 cm^{-1}) by 45 and 46 cm^{-1}. These shifts are larger than those observed previously for HXeCl (27 and 16 cm^{-1}) and HXeBr (37 and 23 cm^{-1}); thus, the matrix effect is stronger for less stable molecules. The results for HXeI are qualitatively different from all previous results on noble-gas hydrides with respect to the frequency order between Ar and Kr matrices. For previously studied HXeCl, HXeBr, and HXeCCH, the H–Xe stretching frequency is reliably (by >10 cm^{-1}) higher in an Ar matrix than in a Kr matrix. In contrast, the H–Xe stretching frequency of HXeI in an Ar matrix is slightly lower than that in a Kr matrix. HXeH absorbs in Ar and Kr matrices at 1203.2 and 1192.1 cm^{-1} (the stronger band for a Kr matrix), respectively. These bands are blue-shifted from the stronger band of HXeH in a Xe matrix (1166 cm^{-1}) by 37 and 26 cm^{-1}, and this frequency order is the same as observed for HXeCl, HXeBr, and HXeCCH but different from HXeI. The present hybrid quantum-classical simulations successfully describe the main experimental findings. For HXeI in the ⟨110⟩ (double substitution) site, the order of the H–Xe stretching frequencies (ν(Xe) < ν(Ar) < ν(Kr)) is in accord with the experimental observations, and also the frequency shifts in Ar and Kr matrices from a Xe matrix are well predicted (30 and 34 cm^{-1}). Both in the theory and experiment, the order of the H–Xe stretching frequencies differs from the case of HXeCl, which suggests the adequate theoretical description of the matrix effect. For HXeH in the ⟨100⟩ (single substitution) site, the order of the frequencies is ν(Xe) < ν(Kr) < ν(Ar), which also agrees with the experiments. The calculated frequency shifts for HXeH in Ar and Kr matrices with respect to a Xe matrix (36 and 23 cm^{-1}) are in a good agreement with the experiments. The present calculations predict an increase of the H–Xe stretching frequencies in the noble-gas matrices with respect to vacuum. © *2015 AIP Publishing LLC.* [http://dx.doi.org/10.1063/1.4906875]

I. INTRODUCTION

Noble-gas hydrides with the general formula HNgY (Ng is a noble-gas atom and Y is an electronegative group) are characterized by an ion-pair character $(HNg)^+Y^-$, which results in a strong IR absorption intensity (~1000 km mol^{-1} or higher) of the H–Ng stretching mode.[1] As an exception, the HXeH molecule does not contain an electronegative fragment.[2] These metastable molecules can be prepared by UV photolysis of a HY precursor in a Ng matrix and subsequent thermal mobilization of the H atoms, which leads to the reaction of the neutral fragments H + Ng + Y → HNgY. Due to weak bonding and large dipole moments, the HNgY molecules are strongly affected by interaction with other species (N_2, CO_2, H_2O, etc.). It is interesting that all experimentally prepared HNgY complexes exhibit blue shifts of the H–Ng stretching mode as compared to the monomers, which has been explained by an increase of the $(HNg)^+Y^-$ charge separation.[3]

In most cases, the HNgY molecules have been studied in Ng matrices (with the same Ng).[1] However, in some studies, the HNgY molecules were prepared in "foreign" matrices, of a different material Ng′ (see Table I).[4–9] It is reasonable to assume that the H–Ng stretching frequency increases with the strength of the interaction of HNgY with the environment. From this point of view, the relatively high frequencies of this mode observed in N_2 and CO_2 matrices are expectable due to the dipole-quadrupole interactions between HNgY and matrix molecules. The lowest frequencies are observed in a Ne matrix, and this can be attributed to a weak interaction of the embedded molecules with the Ne atoms, which is well accepted in matrix isolation.[10] More intriguing is the situation with Ar, Kr, and Xe matrices where the frequency order ν(Xe) < ν(Kr) < ν(Ar) has been observed, which is anomalous with respect to the dielectric constants of the noble-gas solids. Intuitively, the opposite order of the frequencies should take place; at least, the polarizable continuum model (PCM) predicts the opposite order, indeed.[8] The calculations of the 1:1 complexes do not

a)Present address: Department of Applied Chemistry, National Chiao Tung University, 1001 Ta-Hsueh Road, Hsinchu 30010, Taiwan.
b)E-mail address: nakayama@cat.hokudai.ac.jp
c)E-mail address: leonid.khriachtchev@helsinki.fi

TABLE I. Experimental frequencies of the H–Xe stretching mode (in cm^{-1}) of noble-gas hydrides in different matrices.[a]

	Ne	Ar	Kr	Xe	N_2	CO_2
HXeCl	1612	1675	1664	1648		...
HXeBr	1453	1541	1527	1504	1625	1646
HXeCCH	1453	1531	1519	1486	1529.5	...
HXeH	...	...	...	1166	1175	...
HKrCl	...	1482.5	1476	...	...	...

[a]Data from Refs. 2 and 4–9. The strongest bands are presented.

solve the problem either.[6] It becomes clear that the bigger $HNgY@Ng'_n$ systems and more sophisticated computational methods are required for the adequate description of the matrix effect. Concerning HXeH, Tsuge *et al.* have recently suggested based on the experiments in a N_2 matrix that the matrix effect on this molecule should be relatively weak, which is connected with the symmetric structure of this molecule.[8]

The first positive theoretical results have been recently obtained for noble-gas hydrides in different environments. The DFT (B3LYP-D) study done by Cohen *et al.* has been focused on simulations of HXeBr in CO_2 and Xe matrices, and a good agreement with the experimental vibrational spectra has been found for clusters containing 17 matrix particles.[11] Kalinowski *et al.* have performed MP4(SDQ) calculations of HXeCl in noble-gas clusters, and the obtained order of the H–Xe stretching frequencies $\nu(Ne) < \nu(Xe) < \nu(Kr) < \nu(Ar)$ is in agreement with the experiment.[9] Kalinowski *et al.* have suggested that the reason for the frequency order $\nu(Xe) < \nu(Kr) < \nu(Ar)$ is in different stress states of the molecules in the cages due to the different cage sizes. The H–Xe stretching frequencies of HXeCl in all matrix environments are surprisingly found to be red-shifted from the value obtained in vacuum. In another study, Niimi *et al.* have reported hybrid quantum-classical simulations on the vibrational shift of the same molecule HXeCl in different matrices (Ne, Ar, Kr, and Xe) where the interaction energy between HXeCl and surrounding Ng atoms is modeled by the pairwise-additive form.[12] It has been found that the order of the H–Xe stretching frequencies agrees with the experimental order $\nu(Ne) < \nu(Xe) < \nu(Kr) < \nu(Ar)$. On the other hand, the H–Xe stretching frequencies are found to be blue-shifted from the isolated gas-phase value in all matrix environments, which is in contrast to the results by Kalinowski *et al.* It is interesting to note that the two different approaches of Kalinowski *et al.* and Niimi *et al.* lead to the same order of the H–Xe stretching frequency for HXeCl embedded in the four noble-gas solids. The difference between the results of these two studies is the matrix shift with respect to the molecule in vacuum. Summarizing the experimental and theoretical data existing before the present work, this order of frequencies $\nu(Ne) < \nu(Xe) < \nu(Kr) < \nu(Ar)$ seems to be common for noble-gas hydrides.

The present work intends to develop the recent experimental and theoretical success in the studies of noble-gas hydrides in foreign matrices. We prepare HXeI and HXeH in Ar and Kr matrices and compare these results with those in a Xe matrix. These molecules are interesting in several respects. HXeI has one of the weakest chemical bondings among the noble-gas hydrides so that a very strong matrix effect can be expected. HXeH is, in fact, a specific noble-gas hydride because of the absence of the electronegative fragment Y, and the expectations of the matrix effect on this molecule are unclear. It should be mentioned that our attempts to prepare these molecules in a Ne matrix failed. In the present work, the vibrational properties of these systems are successfully modeled by hybrid quantum-classical simulations.

II. EXPERIMENTAL SECTION

A. Experimental details

HI was synthesized by using the method described in Ref. 13. The gas mixtures of HI and argon (≥99.9999%, AGA), krypton (≥99.999%, AGA), and xenon (≥99.999%, AGA) were made by standard manometric procedures in a glass bulb. The HY/Ng gaseous mixtures were deposited onto a cold CsI substrate in a closed-cycle helium cryostat (RDK-408D2, SHI). The IR absorption spectra in the 4000–400 cm^{-1} range were measured with a FTIR spectrometer (Vertex 80V, Bruker) with 1 cm^{-1} resolution co-adding 200 scans. After deposition, the matrices were photolyzed at 3 K by an excimer laser (MSX-250, MPB) operating at 193 nm (~10 mJ cm^{-2}). The mixtures of HBr (≥99%, Aldrich) and noble gases were also used in the experiments. The annealing-induced products were decomposed by a 193-nm excimer laser, a low-pressure mercury lamp, and a 488-nm argon ion laser (model 35-LAS-450, Melles Griot).

B. HXeI and HXeH in a Xe matrix

First, we shortly describe the experiments in a Xe matrix. The HI monomer absorption in a Xe matrix consists of several bands separated by 2–3 cm^{-1}.[14] 600 pulses of 193-nm light (~10 mJ cm^{-2}) decompose practically all HI bands. In the spectrum of the photolyzed and annealed (50 K) HI/Xe (1/1000) matrix (spectrum A in Figure 1), the HXeI bands appear at 1213, 1193.0, and 1186.7 cm^{-1},[4] and HXeH absorbs at 1181.5 and 1165.9 cm^{-1}.[2] Short irradiation at 488 nm (20 s with ~10 mW cm^{-2}) only bleaches the bands of HXeI (spectrum B in Figure 1) whereas the bands of HXeH are quite stable to this radiation. Both HXeI and HXeH are decomposed by a mercury lamp (254 nm) and a 193-nm laser. For a mercury lamp, the decomposition of HXeI is more efficient compared to HXeH. The HXeH bands also appear in the experiments with a HBr/Xe matrix (spectrum C in Figure 1), and no sign of the HXeI bands is naturally observed. Instead, a strong band of HXeBr is observed at 1504 cm^{-1}.[4]

C. HXeI and HXeH in an Ar matrix

HI monomer in an Ar matrix absorbs at 2253.5 and 2245.0 cm^{-1}, in agreement with the literature data.[15] After deposition of HI/Xe/Ar matrices, a new band is observed at 2233.1 cm^{-1} (Figure 2). The relative intensity of this band increases with the Xe concentration and it can be assigned

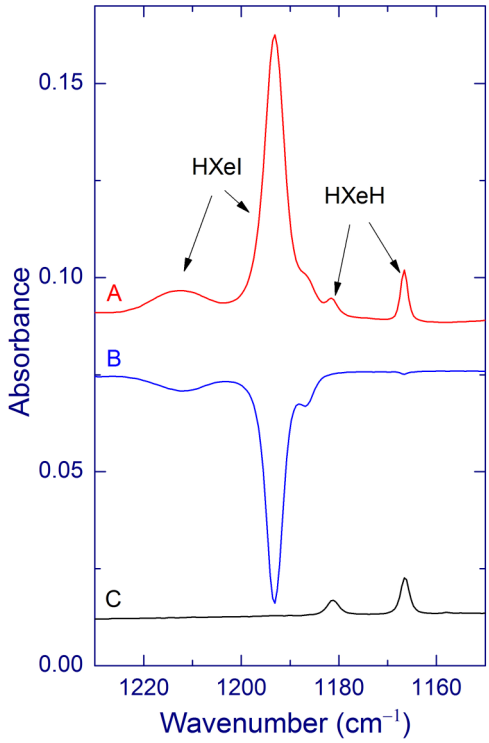

FIG. 1. HXeI and HXeH in a Xe matrix. The FTIR difference spectra show the effects of annealing at 50 K (spectrum A, HI/Xe = 1/1000), irradiation by 488 nm of the annealed matrix (spectrum B, HI/Xe = 1/1000), and annealing at 50 K (spectrum C, HBr/Xe = 1/1000). The shoulder band at 1186.7 cm^{-1} also belongs to HXeI. Prior to annealing, the matrices were photolyzed at 193 nm. All spectra were measured at 3 K.

to the HI···Xe complex (shift of −5 cm^{-1} from the band of non-rotating HI at 2238 cm^{-1}).[15] The assignment for the HI···Xe complex is in agreement with the known calculations predicting a very small frequency shift for this complex.[16]

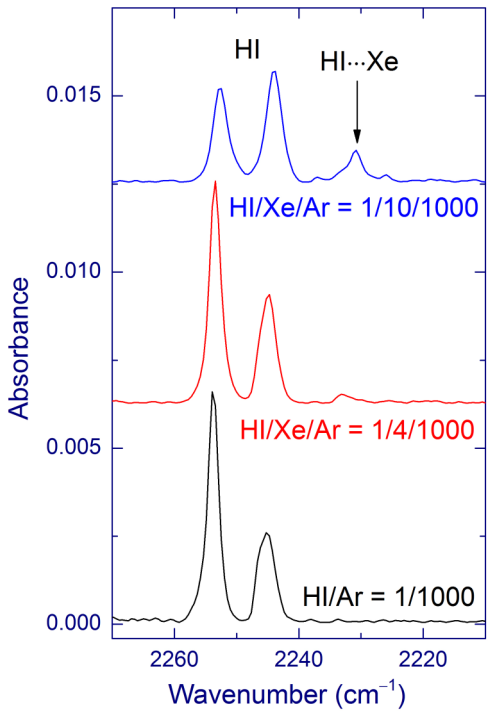

FIG. 2. FTIR spectra of HI/Xe/Ar (1/10/1000, 1/4/1000, 1/0/1000) matrices. The deposition temperature was 15 K. The spectra were measured at 3 K.

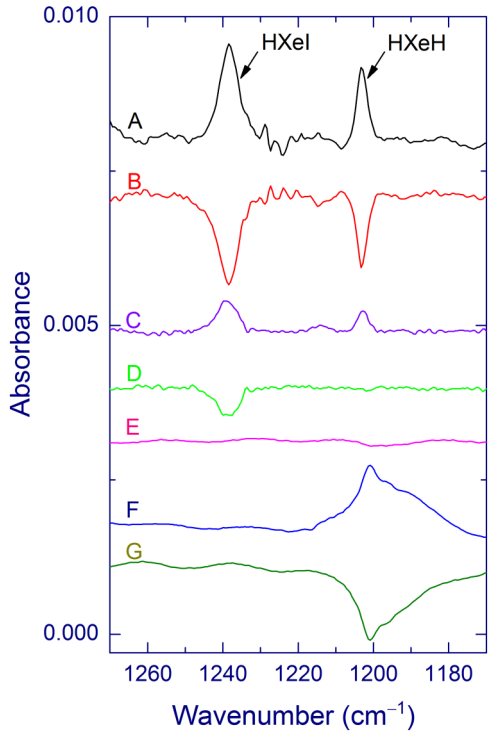

FIG. 3. HXeI and HXeH in an Ar matrix. The FTIR difference spectra show the effects of annealing at 20 K (spectrum A, HI/Xe/Ar = 1/4/1000), irradiation at 193 nm of the annealed matrix (spectrum B, HI/Xe/Ar = 1/4/1000), annealing at 20 K (spectrum C, HI/Xe/Ar = 1/2/1000), irradiation at 488 nm of the annealed matrix (spectrum D, HI/Xe/Ar = 1/2/1000), annealing at 20 K (spectrum E, HI/Ar = 1/1000), annealing at 20 K (spectrum F, HBr/Xe/Ar = 1/4/500), and irradiation at 193 nm of the annealed matrix (spectrum G, HBr/Xe/Ar = 1/4/500). Prior to annealing, the matrices were photolyzed at 193 nm. All spectra were measured at 3 K.

193-nm photolysis decomposes HI producing H and I atoms in an Ar matrix, and some of the iodine atoms are in contact with Xe atoms. Annealing at about 20 K mobilizes the H atoms in an Ar matrix, which should lead to the reaction H + Xe···I → HXeI, similarly to the preparation of other noble-gas hydrides in Ar matrices.[6,8,9] In the spectrum of the photolyzed and annealed HI/Xe/Ar matrices (spectra A and C in Figure 3), two bands appear at 1238.0 and 1203.2 cm^{-1}. The intensities of these bands increase with the Xe concentration and the band shape also slightly changes with the Xe concentration. Without Xe, these bands are absent (spectrum E in Figure 3). These bands are easily decomposed by 193-nm light (spectrum B in Figure 3) and by a mercury lamp, which is characteristic of noble-gas hydrides.

The band at 1238.0 cm^{-1} is assigned to the H–Xe stretching mode of HXeI, and the 1203.2 cm^{-1} band is assigned to the asymmetric stretching vibration of HXeH. There are two arguments for this assignment. First, short irradiation at 488 nm bleaches only the 1238.0 cm^{-1} band (spectrum D in Figure 3), which happens with the HXeI bands in a Xe matrix whereas the bands of HXeH in a Xe matrix are more stable to this radiation as shown above (Figure 1). Second, the 1203.2 cm^{-1} band also appears after photolysis and annealing of a HBr/Xe/Ar matrix (spectrum F in Figure 3) and it is easily decomposed by UV light at 193 nm (spectrum G in Figure 3). The broadness of the HXeH band is probably

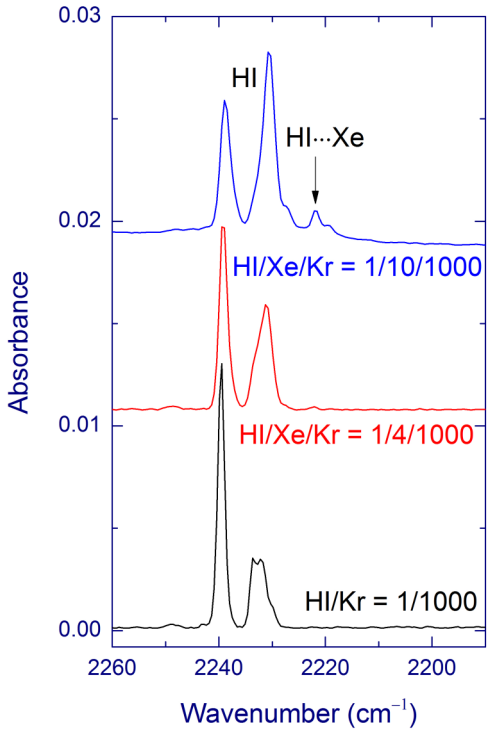

FIG. 4. FTIR spectra of HI/Xe/Kr (1/10/1000, 1/4/1000 and 1/0/1000) matrices. The deposition temperature was 25 K. The spectra were measured at 3 K.

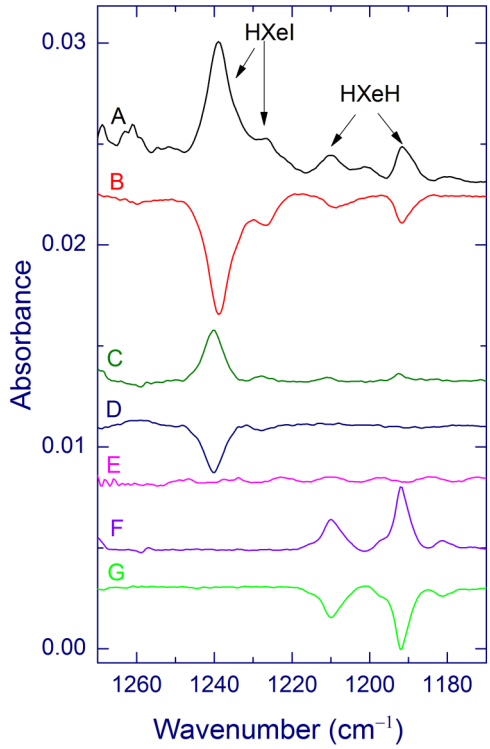

FIG. 5. HXeI and HXeH in a Kr matrix. The FTIR difference spectra show the effects of annealing at 30 K (spectrum A, HI/Xe/Kr = 1/4/1000), irradiation at 193 nm of the annealed matrix (spectrum B, HI/Xe/Kr = 1/4/1000), annealing at 30 K (spectrum C, HI/Xe/Kr = 1/2/1000), irradiation at 488 nm of the annealed matrix (spectrum D, HI/Xe/Kr = 1/2/1000), annealing at 30 K (spectrum E, HI/Xe/Kr = 1/0/1000), annealing at 30 K (spectrum F, HBr/Xe/Kr = 1/4/500), and irradiation at 193 nm of the annealed matrix (spectrum G, HBr/Xe/Kr = 1/4/500). Prior to annealing, the matrices were photolyzed at 193 nm. All spectra were measured at 3 K.

connected with the relatively high Xe concentration in this experiment, which efficiently perturbs the Ar matrix structure. In the last experiment, the intense band of HXeBr in an Ar matrix is observed at 1541 cm^{-1}.[8]

The assignment of the observed bands to the monomeric species should be shortly discussed. Indeed, the matrix after deposition contains some amount of HI dimers and HI···H_2O complexes; thus, the formation of the HXeI···HI and HXeI···H_2O complexes is generally possible. However, there are several arguments that the 1238.0 cm^{-1} band originates from the HXeI monomer. First of all, the HXeI···HI and HXeI···H_2O complexes were studied in a Xe matrix, and their amounts were much lower than those of the HXeI monomer.[17,18] In the present experiments, the HI bands were fully bleached by photolysis whereas the preparation of the HXeI···HI complex needs the I···HI complex as the precursor. The observed shift from the frequency in a Xe matrix (45 cm^{-1}) is more suitable to the matrix effect on the monomer (see Table I) rather than to the complexation effect, for which a larger shift is expected from the experiments in Xe matrices.[17] The latter argument is also applicable to the HXeI···H_2O complex.[18] With respect to HXeH, its complexes do not appear even in a Xe matrix; thus, the formation of these in an Ar matrix is improbable. The study of the HNgY complexes in foreign matrices is a very complicated task, which exceeds the scope of the present work.

D. HXeI and HXeH in a Kr matrix

HI monomer absorbs in a Kr matrix at 2239.5 and 2233 cm^{-1}, in agreement with the literature data.[15] Addition of Xe to a HI/Kr matrix induces a band at 2222.0 cm^{-1} (Figure 4), that increases in intensity with the Xe concentration. This band can be assigned to the HI···Xe complex (shift of −4 cm^{-1} from the band of non-rotating HI at 2226 cm^{-1}).[15,19] This assignment is consistent with the case of an Ar matrix showing a normal matrix shift of this band.

Photolysis of 193-nm decomposes HI producing H and I atoms in a Kr matrix. Annealing above about 27 K mobilizes the H atoms, promoting the formation of noble-gas hydrides.[6,8,20] In the spectrum of photolyzed and annealed HI/Xe/Kr matrices (spectra A and C in Figure 5), we identified four bands at 1239.0, 1227.3 (weak), 1209.9 (weak), and 1192.1 cm^{-1}. Their relative intensities increase with the Xe concentration whereas without Xe, these bands do not appear (spectrum E in Figure 5). These bands are efficiently decomposed by 193 nm light (spectrum B in Figure 5). Short irradiation at 488 nm bleaches only the 1239.0 and 1227.3 cm^{-1} bands (spectrum D in Figure 5). Thus, the 1239.0 and 1227.3 cm^{-1} bands are assigned to the H–Xe stretching mode of HXeI, and the 1209.9 and 1192.1 cm^{-1} bands are assigned to HXeH. The latter two bands are also formed in HBr/Xe/Kr matrices (spectrum F in Figure 5) and easily decomposed by 193 nm light (spectrum G in Figure 5), which confirms our assignment. A weak band at 1181.1 cm^{-1} probably also belongs to HXeH. In the HBr/Xe/Kr experiment, the band of HXeBr in a Kr matrix appears

TABLE II. Equilibrium bond lengths (in Å), harmonic and fundamental (anharmonic) frequencies (in cm^{-1}) of HXeI and HXeH.

	Bond lengths	Harmonic	Fundamental
HXeI	1.769 (HXe)	1354 (H–Xe stretching)	1131 (H–Xe stretching)
	3.001 (Xe–I)	154 (Xe–I stretching)	
		491 (bending)	
HXeH	1.941 (HXe)	1211 (asymmetric)	1138 (asymmetric)
		1095 (symmetric)	
		721 (bending)	

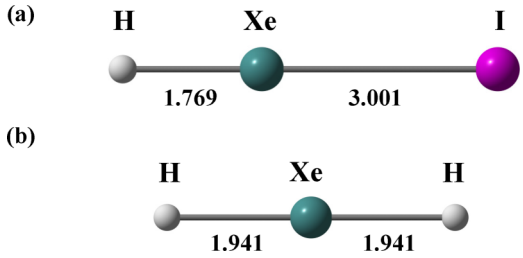

FIG. 6. Equilibrium structures of (a) HXeI and (b) HXeH. The bond lengths are given in Å.

at 1527 cm^{-1}, in agreement with the literature data.[4,8] As discussed earlier, for the case of an Ar matrix, these bands most probably belong to the monomeric species (not to their complexes).

III. COMPUTATIONAL SECTION

A. Computational details

The computational methodology used in the present study is essentially the same as that employed in our previous studies, and the details can be found elsewhere.[12,21] The total potential energy of the system is represented as a pairwise additive form and is given by

$$V_{\text{total}} = V_{\text{HXeY}} + \sum_{i=1}^{N} V_{\text{HXeY}\cdots\text{Ng}_i} + \sum_{i<j}^{N} V_{\text{Ng}_i\cdots\text{Ng}_j}, \qquad (1)$$

where V_{HXeY} is the potential energy of HXeY (Y = I or H) and N is the number of surrounding Ng atoms, $V_{\text{HXeY}\cdots\text{Ng}}$ is the interaction potential energy between HXeY and a Ng atom, and $V_{\text{Ng}\cdots\text{Ng}}$ is that of Ng dimers. The normal coordinates of HXeY are utilized to represent the potential energy of V_{HXeY}, and the interaction energy of $V_{\text{HXeY}\cdots\text{Ng}}$ is determined at each point of the normal coordinates of HXeY. For HXeI, three normal coordinates corresponding to the H–Xe stretching and the doubly degenerate bending vibrations are exploited to represent V_{HXeI}. The Xe–I stretching motion is neglected, and the corresponding normal coordinate is fixed to zero. It has been found that the inclusion of the Xe–I stretching vibration causes a negligible effect on the H–Xe vibrational frequency (~1 cm^{-1}); see also our previous work on HXeCl.[12] For HXeH, the normal coordinates of the asymmetric and symmetric stretching modes are used, while the bending motion is neglected. The inclusion of the bending motion is of course preferable, but it is computationally demanding to perform simulations with this approach because four vibrational modes are involved. In our previous work on HXeCl, the inclusion of the bending motion reduced the H–Xe vibrational frequency by 20-30 cm^{-1} in comparison to the case that neglects the bending motion, but the frequency shifts from the gas-phase values are very similar between these two cases.[12] We expect a similar trend for the simulations of HXeH.

Ab initio calculations by the coupled-cluster singles and doubles including the perturbative contributions of connected triple excitations [CCSD(T)] method are performed to obtain the potential energy surface of V_{HXeI} and also pair interaction energies of $V_{\text{HXeI}\cdots\text{Ng}}$ and $V_{\text{Ng}\cdots\text{Ng}}$. For HXeH, the CCSD(T) method provides a poor description at long distances in the symmetric stretching modes; therefore, the complete active space second-order perturbation theory (CASPT2) method is used to calculate the potential energy surface of V_{HXeH}. The active space for a reference state-averaged complete active space self-consistent field (SA-CASSCF) wavefunction is composed of 10 electrons and 9 orbitals, and the active orbitals include all valence orbitals (H: 1s and Xe: 5s, 5p) and three virtual orbitals belonging to the Xe atom. Note that the pair interaction $V_{\text{HXeH}\cdots\text{Ng}}$ is determined by the CCSD(T) method. The cc-pVQZ basis sets are used for H and I atoms, and the aug-cc-pVQZ basis sets are used for Ng atoms (Ng = Ar, Kr, and Xe). For Kr, Xe, and I atoms, the relativistic pseudopotentials are employed.[22] All *ab initio* calculations have been carried out by the MOLPRO 2010.1 package.[23]

In the calculations of the potential energy surfaces of $V_{\text{HXeY}\cdots\text{Ng}}$, the position of the Ng atom is represented by polar

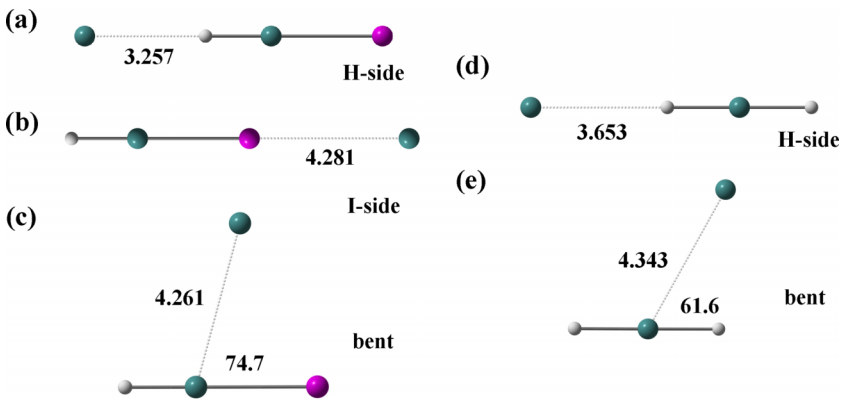

FIG. 7. Minimum energy structures of (a)-(c) HXeI···Xe and (d) and (e) HXeH···Xe complexes where the internal coordinates of HXeI or HXeH are fixed at the equilibrium values shown in Figure 6. The bond lengths are in Å and the angles are in degrees.

TABLE III. Structural parameters (r in Å; θ in deg) of the minimum energy structures of the HXeI···Ng and HXeH····Ng complexes (Ng = Ar, Kr, and Xe).

	H-side	I-side	Bent	
	r(Ng···H)	r(I···Ng)	r(Ng···Xe)	θ(Ng···Xe–Y)[a]
HXeI···Ar	3.159	4.091	3.962	75.2
HXeI···Kr	3.180	4.149	4.074	74.7
HXeI···Xe	3.257	4.281	4.261	74.7
HXeH···Ar	3.487	...	4.033	63.9
HXeH···Kr	3.530	...	4.147	62.7
HXeH···Xe	3.653	...	4.343	61.6

[a]Y = I or H.

coordinates (r, θ, φ), where r is the distance of Ng from the center-of-mass of HXeY, θ is the polar angle measured from the molecular axis of HXeY, and φ is the azimuthal angle measured from the plane of the bending vibration (φ is not required for the HXeH···Ng interaction because the bending motion is neglected for HXeH). The numbers of grid points are $M_r = 25$, $M_\theta = 21$, and $M_\varphi = 4$ for HXeI, and $M_r = 27$ and $M_\theta = 21$ for HXeH.

The potential-optimized discrete variable representation (PO-DVR) method[24] is used to solve the vibrational Schrödinger equations of HXeY in the presence of surrounding Ng atoms. The numbers of optimized basis sets, which are obtained by the solution of the sinc-DVR method for HXeY in the gas phase, are 8 and 6 for the H–Xe stretching and bending motions of HXeI, respectively, and 8 and 6 optimized basis sets are used for the asymmetric and symmetric stretching motions of HXeH, respectively. The convergence of the fundamental (anharmonic) frequency of the H–Xe stretching vibration with respect to the number of optimized basis sets was confirmed by the preliminary calculations.

The simulations of the noble-gas hydrides in matrices are carried out under the periodic boundary condition, and 500 Ng atoms are first placed in a cubic box with the *fcc* lattice structure. Then, the HXeI and HXeH molecules are inserted into this *fcc* lattice by removing a couple of Ng atoms. Three possible orientations in the *fcc* lattice structures are considered for the insertion of HNgY: ⟨100⟩ (four-atomic window), ⟨110⟩ (nearest neighbor), and ⟨111⟩ (three-atomic windows). The number of substituted Ng atoms (N_r) was determined from a sensible choice based on the distance between the adjacent Ng atoms along each orientation. After equilibrating the system, a total of 10^7 Monte Carlo (MC) steps were taken

TABLE IV. Binding energies (in kcal mol^{-1}) of a Ng atom (Ng = Ar, Kr, and Xe) to HXeI and HXeH in the 1:1 complexes.

	H-side	I-side	Bent
HXeI···Ar	0.387	0.466	0.821
HXeI···Kr	0.550	0.631	1.055
HXeI···Xe	0.759	0.810	1.286
HXeH···Ar	0.248	...	0.516
HXeH···Kr	0.339	...	0.643
HXeH···Xe	0.436	...	0.761

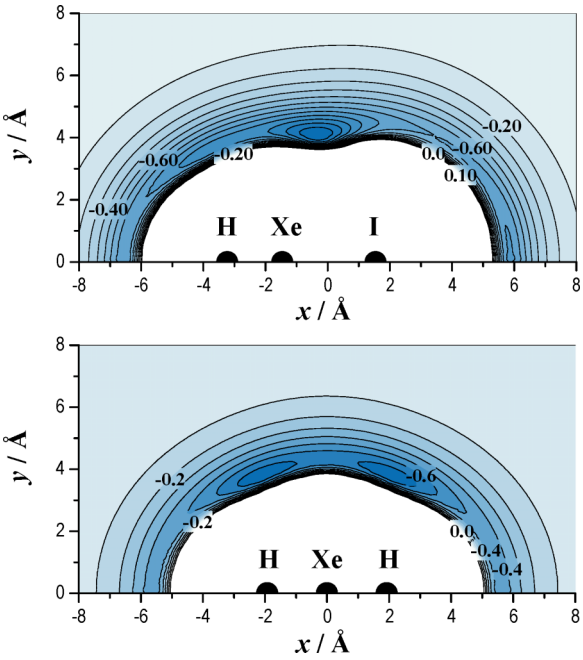

FIG. 8. Two-dimensional contour plots of the potential energy surface (in kcal mol^{-1}) for the HXeI···Xe and HXeH···Xe complexes. The internal coordinates of HXeI and HXeH are fixed at the equilibrium values, and the origins are set to the center-of-mass of HXeI and HXeH. For HXeI, the coordinates of the H, Xe, and I atoms are (−3.232, 0.0), (−1.462, 0.0), and (1.539, 0.0), respectively. For HXeH, the coordinates of the H, Xe, and H atoms are (−1.941, 0.0), (0.0, 0.0), and (1.941, 0.0), respectively.

to obtain statistical averages. The temperatures were set to 15, 20, and 30 K for Ar, Kr, and Xe matrices, respectively, following our previous studies.[12] These temperatures are slightly different from the experimental conditions considered above, but we have found that the peak positions of the H–Xe stretching frequencies do not change significantly as long as the surrounding Ng atoms keep a solid structure.

The stability of different sites was compared by using the stabilization energy defined as

$$\Delta E = \left\langle E^0 + \sum_{i<j}^{N} V_{\mathrm{Ng}_i\cdots\mathrm{Ng}_j} \right\rangle - E^0_{\mathrm{gas}} - N\mu_{\mathrm{Ng}}, \qquad (2)$$

where E^0 is the vibrational ground-state energy of the embedded molecule in the presence of surrounding Ng atoms

TABLE V. Fundamental (anharmonic) frequencies (in cm^{-1}) of the H–Xe stretching frequencies of the HXeI···Ng and HXeH···Ng complexes (Ng = Ar, Kr, and Xe).[a]

	H-side		I-side		Bent	
	Frequency	Shift	Frequency	Shift	Frequency	Shift
HXeI···Ar	1185	+54	1133	+2	1138	+7
HXeI···Kr	1202	+71	1133	+2	1140	+9
HXeI···Xe	1217	+86	1132	+1	1144	+13
HXeH···Ar	1145	+7	...	...	1138	0
HXeH···Kr	1147	+9	...	...	1138	0
HXeH···Xe	1148	+10	...	...	1139	+1

[a]The fundamental frequencies of HXeI and HXeH in vacuum are 1131 and 1138 cm^{-1}, and the frequency shifts from these values are also shown.

TABLE VI. Calculated fundamental (anharmonic) H–Xe stretching frequencies (in cm^{-1}) and stabilization energy (ΔE in kcal mol^{-1}) of HXeI and HXeH in solid Ng matrices (Ng = Ar, Kr, and Xe).[a]

	⟨110⟩				⟨100⟩			
	N_r	Frequency	Shift	ΔE	N_r	Frequency	Shift	ΔE
HXeI								
Ar matrix	2	1357	+226	−8.9	2	1278	+147	−5.1
Kr matrix	2	1361	+230	−11.2	2	1277	+146	−4.4
Xe matrix	2	1327	+196	−11.1	1	1414	+283	−3.2
HXeH								
Ar matrix	2	1151	+13	−3.6	1	1190	+52	−3.2
Kr matrix	2	1162	+24	−3.4	1	1177	+39	−4.5
Xe matrix	2	1152	+14	−2.7	1	1154	+16	−5.9

[a] N_r is the number of Ng atoms substituted with HXeI or HXeH. The frequency shifts from the values obtained in vacuum (HXeI: 1131 cm^{-1}; HXeH: 1138 cm^{-1}) are also shown.

obtained by the PO-DVR method, $\langle\cdots\rangle$ indicates the ensemble average over MC configurations, E^0_{gas} is the vibrational ground-state energy of the embedded molecule in the gas phase, and μ_{Ng} is the chemical potential of Ng atoms. In order to obtain μ_{Ng}, the MC simulations of pure solid Ng atoms (500 atoms) have been performed, and μ_{Ng} is calculated by dividing the ensemble average of total potential energy by the number of Ng atoms in the system.

For each orientation of the substitution site, the MC simulations were initiated with different N_r, and we show only the results for the case of a lower stabilization energy. We have also found that the simulations starting from the ⟨111⟩ site result in the configurations, which are almost identical to those of the ⟨100⟩ site after equilibration; therefore, only the results for the ⟨110⟩ and ⟨100⟩ sites are presented below.

B. HXeY monomers and the HXeY···Ng complexes (Y = I and H; Ng = Ar, Kr, and Xe)

The structural parameters of the equilibrium geometries and the harmonic and fundamental (anharmonic) frequencies of the H–Xe stretching vibration are summarized in Table II (see Figure 6 for the equilibrium structures). For the harmonic frequency of HXeI, good agreement is found with the CCSD(T) calculations by Tsuge *et al.* (1327.2 cm^{-1}).[17] The anharmonic calculation by the DVR approach decreases the H–Xe vibrational frequency by ∼200 cm^{-1}. For HXeH, the equilibrium bond length is in good agreement with the previous calculations,[25–27] but the stretching frequencies are scattered to some extent depending on the computational methods. We find that the asymmetric stretching frequency is decreased by ∼70 cm^{-1} by the treatment of the anharmonic vibrational motion.

Next, we investigate the HXeY···Ng (Y = I and H) complexes with fixed internal coordinates of HXeY. In fact, the intramolecular structures of HXeY are negligibly perturbed upon formation of the HXeY···Ng complexes, and the changes of the bond lengths of HXeY between the monomer and complexes in the fully relaxed configurations are less than 0.003 Å for all complexes. As expected from the previous works,[12,28] three minima have been found for HXeI (Figures 7(a)-7(c)). In two cases, the Ng atom is located at the sides of HXeI in a collinear geometry (H-side and I-side structures) and in the third structure, it is located between and almost equidistant from the Xe and I atoms (bent structure). For the minimum energy structures of the HXeH···Ng complex, the collinear and bent configurations are obtained (see Figures 7(d) and 7(e)). The structural parameters and the binding energies of these complexes are given in Tables III and IV, respectively. In all cases, the strongest interaction is observed for the bent structures. These binding energies are larger than those of Ng dimers (0.274, 0.374, and 0.489 kcal mol^{-1} for the Ar_2, Kr_2, and Xe_2 dimers, respectively).[12] The binding energies of Ng atoms to HXeCl are slightly larger (by 5%–15%) than those to HXeI for the H-side and Y-side structures. For the bent structure, the binding energies of the HXeI···Ng and HXeCl···Ng complexes are very similar. Figure 8 shows two-dimensional contour plots of the potential energy surfaces of the HXeI···Xe and HXeH···Xe complexes where the internal coordinates of HXeI or HXeH are fixed to those of their monomer structures.

The frequency analysis is done for the HXeY···Ng complexes by fixing the positions of Ng atoms at the structures described above, and the results are shown in Table V. The frequencies of the H–Xe stretching vibration are most strongly affected in the H-side structures, whereas the I-side and bent structures have a very small effect on the H–Xe stretching frequency. For the H-side structures, the blue shifts are observed, and this shift increases with the Ng size, and apparently, the order of the frequency (ν(Ar) < ν(Kr) < ν(Xe)) is in disagreement with the experimental results obtained in the matrices. Obviously, larger clusters should be considered for the adequate description, as stated also previously.[6,8]

C. HXeI and HXeH in matrix environments

Hybrid quantum-classical MC simulations were performed for HXeI and HXeH in Ng matrices. For HXeI, the ⟨110⟩ site is reliably lower in energy in all matrices (Table VI). For HXeH, the ⟨110⟩ site is lower in energy only in an Ar matrix whereas in Kr and Xe matrices, the ⟨100⟩ site is energetically favorable. Table VI also shows the H–Xe stretching frequencies calculated for different matrices. In all cases, blue shifts from the band positions obtained in vacuum are observed. These blue shifts can be attributed to the packing effect by the surrounding Ng atoms, mainly from Ng atoms that are close to the hydrogen atom. The shifts observed in matrices are significantly larger than those obtained from the calculations on the 1 : 1 HXeI···Ng and HXeH···Ng complexes (see Table V). The shifts for HXeI are larger than those obtained previously for HXeCl (+119, +116, and +91 cm^{-1} in Ar, Kr, and Xe matrices, respectively).[12]

The contour plots of the two-dimensional distribution functions of Ng (Ng = Ar, Kr, and Xe) atoms around HXeI in the ⟨110⟩ site and HXeH in the ⟨100⟩ sites are shown in Figure 9. Here, the x-axis is taken as the molecular axis of HXeY and r is the radial distance from the x-axis. In the same figure, the positions of Ng atoms in the three minimum energy

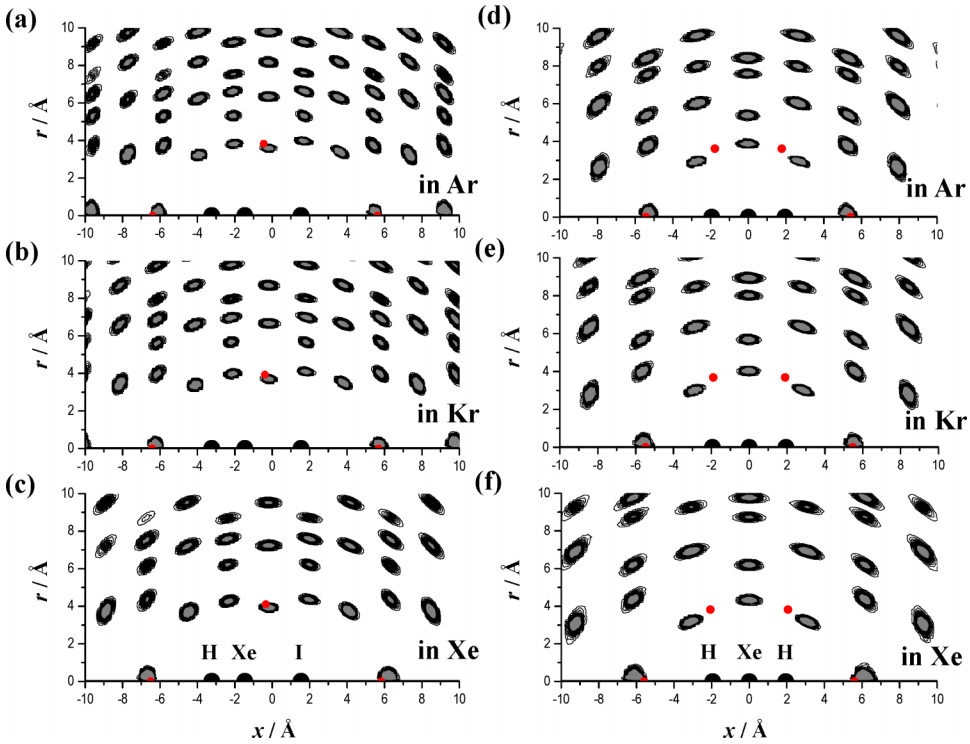

FIG. 9. Contour plots of the two-dimensional distribution functions of Ng atoms around (a)-(c) HXeI in the ⟨110⟩ site and (d)-(f) HXeH in the ⟨100⟩ site in Ar, Kr, and Xe matrices. The positions of HXeI and HXeH in the minimum energy structure in the gas phase are plotted for reference (shown by black circles), and these coordinates are the same as those in Figure 8. The positions of the Ng atoms at the minimum energy structures of the isolated HXeI···Ng and HXeH···Ng complexes are shown by red circles.

structures of the isolated HXeY···Ng complexes (H-side, I-side, and bent structures) are also shown.

IV. CONCLUDING DISCUSSION

We have performed experimental and theoretical studies of HXeI and HXeH molecules in Ar, Kr, and Xe matrices. HXeI exhibits the H–Xe stretching bands at 1238.0 and 1239.0 cm^{-1} in Ar and Kr matrices, respectively. These bands are blue-shifted from the HXeI band observed in a Xe matrix (1193 cm^{-1}) by 45 and 46 cm^{-1}. These shifts are larger than those observed previously for HXeCl (27 and 16 cm^{-1}) and HXeBr (37 and 23 cm^{-1}), which confirms the intuitive expectation that the matrix effect is stronger for less stable molecules. Moreover, it is seen that the results for HXeI are qualitatively different from all previous results with respect to the frequency order between Ar and Kr matrices. For previously studied HXeCl, HXeBr, and HXeCCH, the H–Xe stretching frequency is reliably (by >10 cm^{-1}) higher in an Ar matrix than in a Kr matrix. In contrast, the H–Xe stretching frequency of HXeI in an Ar matrix is slightly smaller than that in a Kr matrix. Evidently, the details of interactions between the embedded molecule and the matrix atoms have changed. Thus, the order of the H–Xe stretching frequencies observed previously for HXeCl, HXeBr, and HXeCCH (ν(Xe) < ν(Kr) < ν(Ar))[4,6,8,9] is not common for noble-gas hydrides.

HXeH absorbs in Ar and Kr matrices at 1203.2 and 1192.1 cm^{-1} (the stronger band is given for a Kr matrix). These bands are blue-shifted from the stronger band of HXeH in a Xe matrix (1166 cm^{-1}) by 37 and 26 cm^{-1}. First of all, the order of these frequencies is the same as observed for HXeCl, HXeBr, and HXeCCH but different from HXeI. More interesting in our opinion is that these shifts are larger than can be expected from the experiments in a N_2 matrix (shift <10 cm^{-1} from a Xe matrix).[8] In contrast, the H–Xe stretching frequency of HXeBr in a N_2 matrix is significantly larger than that in a Xe matrix (Table I).[8] Another remarkable observation is the existence of the second (weaker) band of HXeH in a Kr matrix at 1210 cm^{-1}. In fact, its frequency is higher than that in an Ar matrix following the situation with HXeI rather than with the previously studied HNgY molecules. The interval between the two bands of HXeH in a Kr matrix is about 18 cm^{-1}, i.e., similar to the interval between the two HXeH bands observed in a Xe matrix (15 cm^{-1}).[2] It is possible that the origin of this splitting in Kr and Xe matrices is similar.

The present calculations successfully describe the main experimental findings. For HXeI, the order of the H–Xe stretching frequencies in the ⟨110⟩ (double substitution) site, ν(Xe) < ν(Ar) < ν(Kr), is in accord with the experimental observations, and also the frequency shifts in Ar and Kr matrices from the Xe matrix are well reproduced (experiment: 45 and 46 cm^{-1}; theory: 30 and 34 cm^{-1}). Both in the theory and experiment, the order of these frequencies differs from the case of HXeCl (ν(Xe) < ν(Kr) < ν(Ar));[12] thus, the theoretical model is adequate. In addition, the calculations predict for HXeI stronger shifts between Xe and other matrices than for HXeCl,[12] in agreement with experiment.[4,9]

For HXeH, the ⟨100⟩ (single substitution) site is lower in energy only in Kr and Xe matrices. In an Ar matrix, the ⟨110⟩ (double substitution) site is slightly more preferable. If these sites are considered, the order of the vibrational frequency, ν(Ar) < ν(Xe) < ν(Kr), is theoretically obtained, which partially disagrees with the experiments since the lowest experimental frequency is observed in a Xe matrix. However, the difference in stabilization energy between the ⟨110⟩ and ⟨100⟩ sites for HXeH in the Ar matrix is small

(~0.4 kcal mol^{-1}), compared to those in other matrices. Therefore, if we assume that the trapping site of HXeH is ⟨100⟩ in all matrices, the order of frequencies is ν(Xe) < ν(Kr) < ν(Ar), which agrees with the experiments. The frequency shifts obtained in Ar and Kr matrices with respect to a Xe matrix are in quite good agreement with the experiments (experiment: 37.3 and 26.2 cm^{-1}; theory: 36 and 23 cm^{-1}).

The present calculations can explain only the positions of the stronger bands of HXeH whereas the origin of the weaker bands in Xe and Kr matrices is not fully understood. It is tempting to assign the weaker bands to the second matrix sites obtained theoretically; however, this attempt leads to the contradiction with the experimental band positions. We note that the stabilization energy of HXeH in matrices is small due to the weak interaction with the surrounding Ng atoms, and therefore, there is the possibility that other trapping sites with similar stabilization energies exist. In fact, in the previous study of HXeCl,[12] the trapping sites that could not be classified by the orientation of the *fcc* lattice structure were found although these sites were less stable than the ⟨110⟩ site. If we attempt to assign the weaker bands to other trapping sites, a thorough exploration of the trapping sites is necessary, which is computationally highly demanding. Accurate modelling of matrix sites of HXeH in solid matrices is a challenge for future calculations.

The blue shifts in Ar and Kr matrices with respect to a Xe matrix (~30 cm^{-1}) are obtained in both cases of HXeI in the ⟨110⟩ site and HXeH in the ⟨100⟩ sites. This could partly be explained by the observations that the Ar or Kr atom in the collinear geometry of the H side is found slightly closer to the H atom than that in the minimum energy structures of the HXeI···Ng or HXeH···Ng complexes; in contrast, the Xe atom is slightly displaced outward (see Figure 9). As stated above in the frequency analysis of the HXeI···Ng and HXeH···Ng complexes, the H–Xe vibrational frequency is strongly affected by Ng atoms that are close to the H atom in the collinear geometry. In this situation, a displacement of the Ng atom toward the H atom results in a blue shift because the potential energy curve is quite repulsive when the Ng atom is located closer to the H atom. A similar explanation was suggested by Kalinowski *et al.*[9] This effect is due to different sizes of the Ng lattices where the HNgY molecule is accommodated. It follows that the size of the molecule itself can also contribute to the spectral effect. In accord, a different order of the frequencies is obtained here for HXeI in Ar and Kr matrices compared to the previous results on HXeCl.[12]

The present calculations predict blue shifts of the H–Xe stretching frequencies of HXeI and HXeH in the matrices with respect to vacuum. The same qualitative result was obtained previously for HXeCl.[12] The opposite conclusion was obtained for HXeCl by Kalinowski *et al.* (red shift in the matrices with respect to vacuum).[9] We can note here that the PCM calculations predict blue shifts for these molecules in polarizable medium,[8] in agreement with our hybrid quantum-classical simulations. The DFT (B3LYP-D) calculations by Cohen *et al.* have also featured a blue shift of the H–Xe stretching frequency of HXeBr in a Xe cluster with respect to vacuum.[11] Finally, it is accepted in matrix isolation that the minimal matrix effect (among noble gases) occurs for Ne;[10] thus, the smallest H–Xe stretching frequencies observed for a number of HNgY molecules in Ne matrices (Table I) also suggest blue shifts from the vacuum value for the matrices of the heavier noble gases (Ar, Kr, and Xe). The decisive conclusion on the sign of this shift can be obtained only after experimental observation of these molecules in the gas phase.

The failure to prepare HXeI in a Ne matrix is worth shortly commenting. We have performed a series of calculations of the stabilization energies of HXeI in different matrices employing only the H–Xe stretching motion (neglecting the bending motions). These calculations result in negative stabilization energies for Ar, Kr, and Xe matrices (from −9 to −11 kcal mol^{-1}), which is similar to the results shown in Table VI. In contrast, the stabilization energy of HXeI in a Ne matrix is positive (about +2 kcal mol^{-1}). This positive value of the stabilization energy may be a reason why this molecule does not appear in the experiments in a Ne matrix. There are additional possibilities for this failure such as intrinsic instability of this molecule and/or a relatively high formation barrier. It should be also mentioned that the calculations in a Ne matrix are difficult because the configurations of Ne atoms around the embedded molecule are rather structureless, and the definition of the matrix sites is therefore rather vague.

ACKNOWLEDGMENTS

T.T. and A.N. acknowledge the financial support by KAKENHI (Grant-in-Aid for Scientific Research) from the Ministry of Education, Culture, Sports, Science and Technology (MEXT, Japan). A part of the calculations was performed on supercomputers at the Research Center for Computational Science, Okazaki, Japan. C.Z. thanks the CSC-China Scholarship Council for the Ph.D. grant. M.T. thanks the Academy of Finland for the postdoctoral grant (No. 1139105). This work is also a part of the Project KUMURA of the Academy of Finland (No. 1277993).

[1]L. Khriachtchev, M. Räsänen, and R. B. Gerber, Acc. Chem. Res. **42**, 183 (2009).
[2]M. Pettersson, J. Lundell, and M. Räsänen, J. Chem. Phys. **103**, 205 (1995).
[3]A. Lignell and L. Khriachtchev, J. Mol. Struct. **889**, 1 (2008).
[4]M. Pettersson, J. Lundell, and M. Räsänen, J. Chem. Phys. **102**, 6423 (1995).
[5]M. Lorenz, M. Räsänen, and V. E. Bondybey, J. Phys. Chem. A **104**, 3770 (2000).
[6]H. Tanskanen, L. Khriachtchev, J. Lundell, and M. Räsänen, J. Chem. Phys. **125**, 074501 (2006).
[7]M. Tsuge, S. Berski, R. Stachowski, M. Räsänen, Z. Latajka, and L. Khriachtchev, J. Phys. Chem. A **116**, 4510 (2012).
[8]M. Tsuge, A. Lignell, M. Räsänen, and L. Khriachtchev, J. Chem. Phys. **139**, 204303 (2013).
[9]J. Kalinowski, R. B. Gerber, M. Räsänen, A. Lignell, and L. Khriachtchev, J. Chem. Phys. **140**, 094303 (2014).
[10]M. E. Jacox, Chem. Soc. Rev. **31**, 108 (2002).
[11]A. Cohen, M. Tsuge, L. Khriachtchev, M. Räsänen, and R. B. Gerber, Chem. Phys. Lett. **594**, 18 (2014).
[12]K. Niimi, A. Nakayama, Y. Ono, and T. Taketsugu, J. Phys. Chem. A **118**, 380 (2014).
[13]A. Utsunomiya, K. Sasaki, Y. Tanaka, M. Omura, and N. Tomoshige, U.S. patent 5,693,306 (2 December 1997).
[14]M. Pettersson, L. Khriachtchev, R.-J. Roozeman, and M. Räsänen, Chem. Phys. Lett. **323**, 506 (2000).
[15]M. T. Bowers and W. H. Flygare, J. Chem. Phys. **44**, 1389 (1966).
[16]M. Preller, J. Grunenberg, V. P. Bulychev, and M. O. Bulanin, J. Chem. Phys. **134**, 174302 (2011).

[17]M. Tsuge, S. Berski, M. Räsänen, Z. Latajka, and L. Khriachtchev, J. Chem. Phys. **138**, 104314 (2013).
[18]M. Tsuge, S. Berski, M. Räsänen, Z. Latajka, and L. Khriachtchev, J. Chem. Phys. **140**, 044323 (2014).
[19]A. J. Barnes, H. E. Hallam, and G. F. Scrimshaw, Trans. Faraday Soc. **65**, 3159 (1969).
[20]L. Khriachtchev, M. Saarelainen, M. Pettersson, and M. Räsänen, J. Chem. Phys. **118**, 6403 (2003).
[21]A. Nakayama, K. Niimi, Y. Ono, and T. Taketsugu, J. Chem. Phys. **136**, 054506 (2012).
[22]K. A. Peterson, D. Figgen, E. Goll, H. Stoll, and M. Dolg, J. Chem. Phys. **119**, 11113 (2003).
[23]H.-J. Werner, P. J. Knowles, G. Knizia, F. R. Manby, M. Schütz *et al.*, MOLPRO, version 2010.1, a package of *ab initio* programs, 2010, see http://www.molpro.net.
[24]J. Echave and D. C. Clary, Chem. Phys. Lett. **190**, 225 (1992).
[25]N. Runeberg, M. Seth, and P. Pyykkö, Chem. Phys. Lett. **246**, 239 (1995).
[26]J. Lundell, G. M. Chaban, and R. B. Gerber, J. Phys. Chem. A **104**, 7944 (2000).
[27]T. Takayanagi, T. Asakura, K. Takahashi, Y. Taketsugu, T. Taketsugu, and T. Noro, Chem. Phys. Lett. **446**, 14 (2007).
[28]L. Khriachtchev, A. Lignell, J. Juselius, M. Räsänen, and E. Savchenko, J. Chem. Phys. **122**, 014510 (2005).